Committee 4
Treatment of Non-linear Systems in
Physics and Economics

DRAFT--Sept. 12, 1997
For Conference Distribution Only

MECHANISMS OF SUPERNOVAE EXPLOSIONS: MAGNETOROTATIONAL MODEL AND NEUTRINO EMISSION

by

Guennadi S. Bisnovatyi-Kogan
Main Scientific Researcher
Space Research Institute
Moscow, RUSSIA

The Twenty-first International Conference on the Unity of the Sciences
Washington, D.C. November 24-30, 1997

Mechanisms of supernovae explosions: magnetorotational model and neutrino emission

G.S. Bisnovatyi-Kogan, *

Abstract

Supernovae are the last stage in the eolution of massive stars, following the onset of instability, collapse and formation of a neutron star. Formation of a neutron star is accompanied by a huge amount of energy, approximately 20 % of the rest mass energy of the star, but almost all this energy is released in the form of weakly interacting and hardly registrated neutrino. About 0.1 % of the released neutrino energy would be enough for producing a supernovae explosion, but even transformation of such a small part of the neutrino enegry into the kinetic energy of matter meets serious problems. After 30 years of investigations it was concluded that explosion is impossible in a simple spherically symmetric model. Two variants are investigated for obtaining explosion. In the first one development of convective instability is considered, which lead to increase of the energy of outflowing neutrino, having larger cross- section for interaction with the matter, leading to more effective acceleration. This model is very sensitive to input parameters, to the convection model, leading to controversal results. Accumulation of numerical errors in the process of millions of numerical steps does not give a cirtanity of the explosion in this model until now.

The second model is using transformation of a rotational energy of a rapidly rotating neutron star with its envelope into the energy of explosion due to action of a magnetic field as a transformation

*Space Research Institute, Russian Acadamey of Sciences, Moscow, Russia

mechanism. Calculations in this model in 1 and 2 dimensions give a stable value of transformation of the rotational energy into the energy of explosion on the level of few percents. This occures to be enough for explanation of the energy release in supernova explosion. The last model gives a direct demonstration of nonlinear interaction between hydrodynamical and hydromagnetic systems. At first a field is amplified by differential rotation, then this enhanced field leads to transformation of the rotational energy into the energy of explosion. After that the magnetic field is returning to its initial poloidal configuration and stellar rotation becomes rigid and rather slow.

1 Introduction

Supernova explosions are the most spectacular events in the universe of stars. The major part of energy releases in a time interval (< 1 s) small relative to not only stellar but also human lifetime, whereas its quantity exceeds by an order of magnitude and more the energy emitted by the star over its total lifetime reaching $\sim 10^{10}$ years for Sun-like stars. During the neutron star formation most of the energy releases in the form of scarcely observable neutrinos.

A supernova explosion is the end of the life of most massive stars with $M > 8M_{\odot}$. The flash itself results either from the thermal instability development in degenerate core, or from gravitational and partly nuclear energy release during collapse which leads to the neutron star formation. The rotation and magnetic field may play an important role in conversion of gravitational energy into energy of observable flash. A small part of stars (the most massive ones) seem to end their life with collapse and black hole formation. The collapse in this case may be "silent" and not lead to supernova explosion.

From observational point of view, supernovae fall into Type I (SNI) with no hydrogen lines in their emission spectrum and numerous absorption lines of various heavy elements instead, and Type II supernovae (SNII) with much hydrogen and nearly normal chemical composition. Type I SN are divided into 3 groups, two of which, SN Ib,c are substantially different from SN Ia. SNII have been established to be a result of the evolution of massive stars, while SNI have less massive stars for progenitors; many SNI are likely to occur in binaries.

The pulsars are thought to be produced by SNII explosions. The common

feature between SN II and SN Ib,c is a nonthermal radioemission visible during several years after explosion. This is a real indication, that SN Ib,c also give birth to pulsars. Contrary, SN Ia never show such kind of radioemission, so it is suggested that they are produced by nuclear explosions, leading to total disruption of the star, while other types of SN result from hydrodynamical collapse, leading to formation of a neutron star. In SN II the collapsing core is surrounded by large hydrogen envelope, while in SN Ib,c the collapsing core is almost naked, presumably originated from less massive stars, which have lost its hydrogen-rich envelope in preceding evolution, may be in a binary.

The presence of hydrogen in the SNII spectra gives evidence that the explosion occurred before the star has lost its hydrogen envelope. The shape of the light curve shows that prior to the explosion this envelope could be extremely extended, $(10^3 \div 10^4) R_\odot$ [18]. Observation in the Large Magellanic Cloud of SN1987A, the first visible by the naked eye for more than 300 years supernova, provide evidence for a SNII explosion in a fairly compact blue supergiant. The SN1987A light curve may be reproduced only in the case of a prolonged energy release after the main explosion. The variety of SNII light curves is substantially larger than of SNI [38].

The exact relationship between SNI and SNII, on the one hand, and the initial stellar masses, mechanisms of explosion and resulting remnants, on the other, is not reliably established. New observational data may change some of our present model conceptions. Various aspects of the supernova problem arising from observations and their interpretation are given in the book [37].

The physical processes accompaning supernovae explosions are: nuclear reactions, neutrino processes, convection; equation of state of matter in wide region of parameters, where effects of degeneracy and relativistic corrections are important, are described in the book [6] Despite many efforts, the supernova theory is far from complete even in spherically symmetrical approximation by reason of serious numeric and fundamental difficulties related to non-stationary convection, neutrino transport and equation of state for matter of a density above the nuclear.

2 Hydrodynamical theory of supernovae

Iron cores with mass $M_{Fe} \geq 1.4\,M_\odot$ lose their stability through the iron dissociation which directly leads to a rapid collapse. The neutronization rate and time interval in which the contraction proceeds with β-decay rate increase with decreasing mass. The iron core forms in stars with initial mass $M_i > 10M_\odot$, while for $M > 13M_\odot$ all stages of nuclear burning proceed smoothly. As all evolutionary calculations yield significant uncertainty in the relationship $M_{Fe}(M_i)$, the stability loss due to the iron dissociation is certain for single stars with $M_i > 13 \pm 3M_\odot$.

Hydrodynamical calculations of iron core collapse have been first performed in [14], and soon after in [19], [4]. Hydrodynamical equations have been solved and, massive stellar cores ($M \geq 2M_\odot$) on the boundary of hydrodynamical stability have been taken for initial conditions. These studies concern the effect of electron and muon neutrinos on collapse, the role of neutrino deposition leading to the envelope heating and probable ejection, and the effect of burning of thermonuclear fuel ^{12}C, ^{16}O remaining around the iron core. It has been noted in [9] that the reflection of infalling matter from the surface of stable neutron star and formation of a shock wave (bounce) may also be important for producing supernova explosion. Numerous calculations to date (see reviews [18], [40],[41],[10],[17]) have revealed sensitivity of the results to the equation of state of nuclear matter, quantity of remaining thermonuclear fuel, treatment of convection. The results are strongly, influenced by adopted methods for including neutrinos at transparent and opaque stages. Calculations including neutrino processes in a self-consistent way over the entire star were first performed by D.K. Nadyozhin [31],[32]. It was shown that promoting the conversion of kinetic energy into heat and eliminating the bounce almost completely is the major effect of neutrinos. The mean energies of neutrinos arising in collapse are $\sim$ 10 MeV[1] , and their deposition is insufficient to reverse envelope collapse and to obtain a powerful explosion. Inclusion of thermonuclear burning of oxygen in the envelope, muon- and tau-neutrinos, momentum transfer from neutrinos to nuclei caused by coherent scattering due to neutral currents does almost not alter the results.

[1] in [28], the mean energies of electron neutrinos equal 14 MeV, electron antineutrinos, 15 MeV, other neutrino species (ν_μ, $\tilde{\nu}_\mu$, ν_τ, $\tilde{\nu}_\tau$), 32 MeV. The total energy of emitted neutrinos $\sim 6 \times 10^{53}$ erg is distributed almost equally between these six types of particles.

2.1 Convective instability in collapsing stellar cores.

To maintain the neutrino energy flux out of the core, the concentrations of leptons in the region of neutrinosphere falls abruptly outward, following the drop in pressure. This leads to the convective instability development [15] since the element motion inward is related to an excess of the element density over that of surroundings for the pressure to be compensated, and vice versa. Convective motions in the neutrinosphere might bring hot material outward and increase the mean energy and flux of escaping neutrinos whose deposition could initiate an explosion.

The possibility for such an instability to develop and its consequences have been analyzed in [24],[25]. An equilibrium equation of state of a hot dense matter [22] with neutrinos in thermodynamical equilibrium has been used. The convective instability investigation have led to the conclusion that within the neutrinosphere, at $dx_l/dr < 0$ (x_l is the fractional concentration of leptons), the convection development is possible only at $\gamma_l = \left(\frac{\partial S}{\partial x_l}\right)_{\rho,P} < 0$, if the entropy does not decrease with radius and, consequently , has no destabilizing effect. Studying the shock motion inside the neutrinosphere reveals that the entropy in the post-shock region really increases with decreasing density. Calculating γ_l from the equation of state in [22] shows that at high T and ρ insuring a purely nucleon composition, the value $\gamma_l > 0$, so the convection development is hardly possible at $\rho > 10^{14}$ g cm^{-3}. In the region transparent to neutrino at $\rho < 10^{12}$ g cm^{-3} the lepton fractional concentration increases outside due to increase in electron fraction and lepton gradient will tend to stabilize these regions against convective overturn. Thus lepton driven overturn is possible only at densities $10^{12} < \rho < 10^{14}$ g cm^{-3}, where neutrino trapping occures, and $\gamma_l < 0$. Account of convection in local approximation in hydrodynamic calculations has shown that the degree of enhancement of neutrino flux is ambiguous and the possibilities for obtaining an explosion remain doubtful [24].

2.2 2D and 3D calculations of neutrino convection.

An unstable lepton and entropy profiles formed after $\sim$ 10 ms of the creation of shock wave and bounce of the core, can drive a violent Reyleigh- Taylor-like overturn studied in [12]. Coupling 2-D hydrodynamics treated by precise-parabolic method (PPM), with independent 1-D neutrino transport were

used. The explosion was obtained in this model, while without neutrino transport, or with account of convection in 1-D hydrodynamical model the explosion did not happen. Extended calculations in similar model with 2-D neutrino transport have been presented in [13]. Here convection becomes so violent, that spherical and even plane symmetry of the core are strongly broken, neutrino emission and mass ejection goes anizotropically, inducing the explosion with ejection of few tens of high entropy clumps, and giving a kick to a neutron star, which by estimations can reach a speed of $\sim$ 500 km/s.

3-D simulations of convection in the shocked matter of the supernova core have been done in [36], assuming that the neutrino radiation from the proto-neutron star is radial, but axisymmetric. the asphericity of the neutrino flux was connected with rapid rotation of the protoneutron star. The formation of high-entropy hot bubbles and jet-like explosion was obtained as a result, but explosion energy problem was not considered.

PPM method was used in 2-D calculations [20],[21] of neutrino-driven supernova with convective overturn and accretion. The effects of convection obtained here are less pronounced then in [13], while powerful explosion is obtained in a certain, although rather narrow window of core ν fluxes in which one-dimensional models do not explode. The maximum attainable velocities of the kick are estimated to be around 200 km/s.

Extensive 2-D study of supernova explosion following the collapse of cores of two massive stars (15 and $25M_{\odot}$) have been performed in [16]. The calculations begin at the onset of core collapse and stop several hundreds milliseconds after the bounce, at which time seccessful explosion of appropriate magnitude have been obtained. The explosion is powered by the heating of the envelope due to neutrino emitted by the protoneutron star. This heating generates strong convection outside the neutrinosphere which was demonstrated to be critical to the explosion. Convection leads to violation of radiative equilibrium between neutrino emission and absorption. Thus explosions become quite insensitive to the physical input parameters, such as neutrino cross-section or nuclear equation of state parameter.

Smooth particle hydrodynamics (SPH) code was used for 2-D calculations with spherically symmetric gravity and realistic equation of state. 2-D explicit code for neutrino transport was developed with account of most important processes of neutrino emission, absorption and scattering. A peculiar characterictic of neutrino processes in supernova is that dominant pro-

cess wich leads to neutrino trapping does not affect the neutrino spectrum, because elastic scattering between nucleons and neutrinos happens almost without the energy exchange. That leads to the situation, where the optical depth can be large without thermalizing the fields. As a result, local thermodynamic equilibrium cannot be assumed.

The main features common to all 2-D simulations made in [16] are following. After an initial period of dynamical infall lasting a few hundreds milliseconds, the central density becomes supernuclear, the core hardens and a bounce shock is launched. Within a few milliseconds this shock stalls due to energy losses at a radius $\sim$ 150 km. At this point 2-D calculations begin to differ greatly from 1-D computations because of the onset of hydrodynamical instabilities. Most important to the supernova is the neutrino-driven convection that lasts for over 100 ms until a successful explosion is achieved.

Investigations of collapse and explosion of rotating cores have shown, that the explosion proceeds in the same manner as in the nonrotating case, exept the rotation has a strong influence on the shape of the convective patterns that develope above the protoneutron star. As was pointed in [16], the most wanting aspect of the calculations remains in neutrino physics, because of the obvious difficulties of radiation transport in multidimensions. The basic flux-limited approximation leaves much to be desired in nearly optically thin regions, and also nonelastic neutrino nucleus interactions have been ignored, which could play an important role in the explosion. As was indicated in [16], at a time $\sim$ 200 ms SPH model ceased to adequately resolve the atmosphere above the neutron star and simulations had to be stopped. The fact the this time is close to the time of the formation of the successful explosion shock make it desirable to check more carefully the role of numerical effects in these calculations. Another variant of 2-D calculations with similar input physics, but different numerical scheme and initial conditions have been performed in [30], and no explosion was obtained in presence of the neutrino-driven convection.

3 Magnetorotational model of supernova explosion

When all the above mechanisms of explosion prove inefficient, the magnetic field may convert the rotational energy of a neutron star resulting from collapse into kinetic energy of the envelope and thus ensure a supernova explosion. A magnetorotational model of explosion has been suggested in [5][2]. Numerical calculations for this model have been made to cylindrical approximation in [9], [1], spherically symmetric approximation in [29] and in a simplified two-dimensional formulation in [35]. The results of these calculations are in qualitative agreement and give a conversion of $\sim 3\%$ of the rotational energy into kinetic energy of the outburst. For $E_{rot} = 10^{53}$ erg we have the energy $E_{kin} = 3 \times 10^{51}$ erg sufficient to account for a supernova explosion.

3.1 Mechanism of magnetorotational explosion.

When a rapidly rotating presupernova collapses, it leads to formation of a rapidly rotating neutron star surrounded by a differentially rotating envelope in which the centrifugal forces are comparable with gravitational ones. The differential rotation twists the lines of magnetic force, thereby causing the magnetic field with initial energy $\epsilon_M \ll \epsilon_G$ to increase linearly in time. When the energy of the field in the envelope approaches $\epsilon_M \sim \epsilon_G$, the magnetic pressure pushes the material outward. The arising wave of compression propagates over medium with falling density, gets enhanced and transforms into shock to result in a powerful explosion. As the compression wave and subsequent shock move outward, their energy keeps increasing, maintained by rotational energy supplied by magnetic field. The magnetic field serves also to transfer to outer layers an essential part of the total angular momentum. Calculation of collapse for rotating star with a very strong initial magnetic field $\epsilon_M \sim \epsilon_G$ have been done in [26]. The obtained picture of an explosion in the form of outbursts lined up along the dipole axis differs from the magnetorotational explosion where the major part of the outburst occurs in the equatorial plane. The initial magnetic fields in [26] exceed 3 -4 orders

[2]Observations of radio emission at a relatively early period of the flash, roughly one year after the light peak, provide an indirect evidence for an essential role played by the magnetic field in supernova explosion [39].

of magnitude the really observed ones.

3.2 Basic equations.

The equations of magnetohydrodynamics (MHD) with gravitation in cylindrical Eulerian system (r, φ, z), at an infinite conductivity and axial symmetry $\partial/\partial\varphi = 0$ read [23]

$$\begin{aligned}
\frac{\partial v_r}{\partial t} &+ v_r \frac{\partial v_r}{\partial r} + v_z \frac{\partial v_r}{\partial z} - \frac{v_\varphi^2}{r} = -\frac{1}{\rho}\frac{\partial P}{\partial r} - \frac{\partial \varphi_G}{\partial r} \\
&+ \frac{1}{\rho c}\left(j_\varphi B_z - j_z B_\varphi\right), \qquad (1) \\
\frac{\partial v_\varphi}{\partial t} &+ v_r \frac{\partial v_\varphi}{\partial r} + v_z \frac{\partial v_\varphi}{\partial z} + \frac{v_r v_\varphi}{r} = \frac{1}{\rho c}\left(j_z B_r - j_r B_z\right), \qquad (2) \\
\frac{\partial v_z}{\partial t} &+ v_r \frac{\partial v_z}{\partial r} + v_z \frac{\partial v_z}{\partial z} = -\frac{1}{\rho}\frac{\partial P}{\partial z} - \frac{\partial \varphi_G}{\partial z} \\
&+ \frac{1}{\rho c}\left(j_r B_\varphi - j_\varphi B_r\right), \qquad (3) \\
\frac{\partial \rho}{\partial t} &+ v_r \frac{\partial \rho}{\partial r} + v_z \frac{\partial \rho}{\partial z} + \rho\left[\frac{1}{r}\frac{\partial (r v_r)}{\partial r} + \frac{\partial v_z}{\partial z}\right] = 0, \qquad (4)
\end{aligned}$$

$$\begin{aligned}
\frac{\partial B_r}{\partial t} &= -\frac{\partial}{\partial z}\left(v_z B_r - v_r B_z\right), \qquad (5) \\
\frac{\partial B_\varphi}{\partial t} &= \frac{\partial}{\partial z}\left(v_\varphi B_z - v_z B_\varphi\right) - \frac{\partial}{\partial r}\left(v_r B_\varphi - v_\varphi B_r\right), \qquad (6) \\
\frac{\partial B_z}{\partial t} &= \frac{1}{r}\frac{\partial}{\partial r}\left[r\left(v_z B_r - v_r B_z\right)\right], \qquad (7) \\
&\frac{1}{r}\frac{\partial}{\partial r}(r B_r) + \frac{\partial B_z}{\partial z} = 0, \qquad (8) \\
j_r &= -\frac{c}{4\pi}\frac{\partial B_\varphi}{\partial z}, \qquad (9) \\
j_\varphi &= \frac{c}{4\pi}\left(\frac{\partial B_r}{\partial z} - \frac{\partial B_z}{\partial r}\right), \qquad (10) \\
j_z &= \frac{c}{4\pi r}\frac{\partial}{\partial r}(r B_\varphi), \qquad (11)
\end{aligned}$$

$$\frac{1}{r}\frac{\partial}{\partial r}\left(r\frac{\partial \varphi_G}{\partial r}\right)+\frac{\partial^2 \varphi_G}{\partial z^2}=4\pi G\rho, \tag{12}$$

$$\frac{\partial E}{\partial t}+v_r\frac{\partial E}{\partial r}+v_z\frac{\partial E}{\partial z}+\frac{P}{\rho}\left[\frac{1}{r}\frac{\partial (rv_r)}{\partial r}+\frac{\partial v_z}{\partial z}\right]=-f_\nu, \tag{13}$$

$$P=P(\rho,T),\quad E=E(\rho,T),\quad f_\nu=f_\nu(\rho,T), \tag{14}$$

Here equation (1)–(3) are the equations of motion with magnetic fields, (4) is the continuity equation, (5)–(7) are the "frozen-in" field equations ($\partial\vec{B}/\partial t=\mathrm{rot}(\vec{v}\times\vec{B})$), (8) is the equation for a field with no divergence ($\mathrm{div}\vec{B}=0$), (9)–(11) are the equation for field generation by electric currents (with no term for displacement currents, $\mathrm{rot}\vec{B}=\frac{4\pi}{c}\vec{j}$), (12) is the Poisson's equation, (13) is the energy equation, $\vec{v}(v_r,v_\varphi,v_z)$ is the velocity, $\vec{B}(B_r,B_\varphi,B_z)$ is the magnetic field strength, $\vec{j}(j_r,j_\varphi,j_z)$ is the current density, c is the velocity of light, φ_G is the gravitational potential.

Under assumption of a plane symmetry the set of equations (1)–(4) is solved for a star of mass M at the following boundary conditions:

$$\begin{aligned}
&\text{(a) } P &&= \rho=T=B_\varphi=0 && \text{on the outer boundary}\\
&\text{(b) } v_r &&= j_r=B_r=0 && \text{at r = 0}\\
&\text{(c) } v_\varphi &&= j_\varphi=B_\varphi=0 && \text{at r = 0}\\
&\text{(d) } v_z &&= 0,\ \frac{\partial j_z}{\partial z}\ \text{or}\ j_z=0,\ \frac{\partial B_z}{\partial z}\ \text{or}\ B_z=0 && \text{at z = 0}
\end{aligned} \tag{15}$$

The dissipative processes are neglected in calculations, the neutrino emission is allowed for by f_ν, an artificial viscosity is used for shock calculations. The introduction of artificial viscosity in [2], where a Lagrangian coordinate system is used, implies replacing P in the equations of motion (1)–(3) and energy (13) by

$$P+\omega_1=P-\nu\mathrm{div}\vec{v}=P-\nu\left[\frac{1}{r}\frac{\partial (rv_r)}{\partial r}+\frac{\partial v_z}{\partial z}\right], \tag{16}$$

where ν is the viscosity coefficient. The distributions $\rho(\vec{r})$, $T(\vec{r})$, $\vec{B}(\vec{r})$ are specified at initial time, and the last of them should satisfy the condition of the absence of magnetic charges (8) and yield finite values of $\vec{j}(\vec{r})$ throughout the star, in accordance with (9)–(11). Surface and linear currents arising from

singularities in $\vec{j}(\vec{r})$ are usually ignored in calculations. If the equality (8) does hold at the beginning, it will remain valid with time provided that only equations (5)–(7) are used to determine the field.

3.3 Cylindrical approximation.

A cylinder uniform along the z-axis with $v_z = B_z = j_r = j_\varphi = 0$ is considered in a one-dimensional formulation. It means that in a real star the motion along the $z - axis$ is neglected. The basic equations with the Lagrangian independent variable

$$s = \int_0^r \rho' r' dr' \tag{17}$$

become [9], [1]

$$\frac{\partial}{\partial t}\left(\frac{1}{\rho}\right) = \frac{\partial}{\partial s}(r v_r), \quad \frac{\partial r}{\partial t} = v_r, \quad \frac{\partial \varphi}{\partial t} = \frac{v_\varphi}{r}, \tag{18}$$

$$\frac{\partial v_r}{\partial t} - \frac{v_\varphi^2}{r} = -r\frac{\partial P}{\partial s} - \frac{1}{8\pi r}\frac{\partial}{\partial s}(rB_\varphi)^2 + g. \tag{19}$$

$$\frac{\partial}{\partial t}(r v_\varphi) = \frac{rB_r}{4\pi}\frac{\partial}{\partial s}(rB_\varphi), \tag{20}$$

$$\frac{\partial}{\partial t}\left(\frac{B_\varphi}{\rho r}\right) = rB_r\frac{\partial}{\partial s}\left(\frac{v_\varphi}{r}\right), \quad rB_r = A = \text{const} \tag{21}$$

$$\frac{\partial E}{\partial t} = -P\frac{\partial}{\partial s}(r v_r) - f_\nu, \tag{22}$$

$$g = -2G\frac{2\pi(M_0 + s)}{r}. \tag{23}$$

Here M_0 is the mass per radian of a unit length of a core with a uniform solid-body rotation, g is a gravitational acceleration. An approximate equation of state in the form

$$P = \begin{cases} 3.09 \times 10^{12}\rho^{5/3}\frac{1+1.59\times10^{-3}\rho^{1/3}}{\left(1+3.18\times10^{-3}\rho^{1/3}\right)^2} \\ +6.5 \times 10^4\rho^2 + aT^4/3 + \rho\mathcal{R}T \quad \text{for } \rho < 3 \times 10^9 \text{ g cm}^{-3} \\ 2.04 \times 10^{27} + 6.5 \times 10^4\rho^2 \\ +aT^4/3 + \rho\mathcal{R}T \quad \text{for } \rho \geq 3 \times 10^9 \text{ g cm}^{-3} \end{cases} \tag{24}$$

$$E = \begin{cases} \frac{4.635\times10^{12}\rho^{2/3}}{1+3.18\times10^{-3}\rho^{1/3}} + 6.5\times10^{4}\rho \\ +\frac{aT^4}{\rho} + \frac{3}{2}\mathcal{R}T & \text{for } \rho < 3\times10^{9} \text{ g cm}^{-3} \\ 5.19\times\frac{10^{27}}{\rho} + 2.41\times10^{18}\left(\rho - 3\times10^{9}\right)/\rho \\ +6.5\times10^{4}\rho + \frac{aT^4}{\rho} + \frac{3}{2}\mathcal{R}T & \text{for } \rho \gg 3\times10^{9} \text{ g cm}^{-3} \end{cases} \tag{25}$$

has been used in [9], [1]. The equation allows approximately for the transition from non-relativistic to relativistic electrons occuring at a strong degeneration. The electron pressure has been taken to be constant after the onset of neutronization. Neutrino losses due to URCA-processes has been taken into account.

At initial time $t = 0$ it has been adopted $T = 0$, and the density distribution has been specified in the form [1]

$$\rho(s,0) = a\exp\left[-b(r-R_0)^2\right]; \quad a,b = \text{const.} \tag{26}$$

Here $R_0 = R(0,t)$ is the core radius; M is the envelope mass per unit length per radian. It is adopted $v_r(s,0) = 0$, $B_\varphi(s,0) = 0$, and the boundary conditions (38.15a). Also specified are the constant A from (21) and the initial distribution $v_\varphi(s,0)$ from the radial equilibrium equation (19) with $\partial v_r/\partial t = 0$

$$\frac{v_\varphi^2(s,0)}{r(s,0)} - r(s,0)\frac{\partial}{\partial s}P(s,0) + g(s) = 0. \tag{27}$$

The angular momentum of the system core+envelope is assumed to conserve throughout the calculations; the relation for this conservation, owing to the continuity of v_φ on the core boundary, is written in the form of the boundary condition

$$\frac{M_0}{2}\frac{\partial h}{\partial s} - h = 0 \ \text{ at } \ s = 0, \qquad h = rB_\varphi \tag{28}$$

3.4 Calculational results.

The problem was calculated numerically in the region

$$t > 0, \quad 0 < s < M \quad (R_0 < r < R(t)). \tag{29}$$

The basic dimensionless parameters of the problem are

Figure 1: The distribution over the dimensionless parameter s of the temperature T and angular velocity Ω normalized to their maximum dimensionless values $T^* = 64.6$ and $\Omega^* = 1$ at various times for $\alpha = 0.01$. All curves are labeled by corresponding times t_α, from [1].

$$\alpha = \frac{A^2}{4\pi M V_0^2}, \qquad \left(V_0 = \sqrt{2\pi G M_0},\right), \quad \beta = \frac{M_0}{M}. \tag{30}$$

The solution in [1] was obtained for $\beta = 1$, $\alpha = 10^{-2}, 10^{-4}, 10^{-8}$. In order to introduce dimensionless quantities, all the variables are taken in the form $F = F_0 \tilde{F}$ with the following scale variables F_0:

$$\begin{aligned} v_0 &= V_0, \quad r_0 = R_0, \quad t_0 = R_0/V_0, \quad h_0 = A, \quad \rho_0 = M/R_0^2, \\ P_0 &= MV_0^2/R_0^2, \quad E_0 = V_0^2, \quad \Omega_0 = V_0/R_0 \quad (\Omega = v_\varphi/r), \\ s_0 &= M, \quad T_0 = V_0^2/10^3\mathcal{R}, \quad f_{\nu 0} = V_0^3/R_0; \text{ with} \\ R_0 &= 10^6 \text{ cm}, \quad 2\pi M_0 = 0.5 \times 10^{-6} M_\odot. \end{aligned} \tag{31}$$

Decreasing the parameter α causes the timescales of processes to increase as $\alpha^{-1/2}$. As $\alpha \to 0$, it is convenient to introduce the dimensionless functions

$$t_\alpha = t\alpha^{1/2}, \quad v_{r\alpha} = v_r \alpha^{-1/2}, \quad h_\alpha = h\alpha^{1/2}, \quad f_{\nu\alpha} = f_\nu \alpha^{-1/2}, \tag{32}$$

having the same relationships between them for all small α. For other functions $F_\alpha = F$. The results of numerical calculations are presented in Figures 1–4 from [1].

Propagation of a slow ($v < v_A = B\sqrt{4\pi\rho}$) MHD shock over the envelope may be seen in Fig.1. The region of the sharp temperature peak beyond

Figure 2: The shape of lines of magnetic force in a region nearby the core at time $t_\alpha = 7$ for $\alpha = 0.01$ (dashed line) and $\alpha = 10^{-4}$ (solid line), from [1].

Figure 3: Neutrino luminosity $q_\alpha = \int_0^1 f_{\nu\alpha}\, ds$ as a function of time t_α, normalized to the maximum dimensionless value $q_\alpha^* = 1.4$ for $\alpha = 0.01$ (dashed line) and $\alpha = 10^{-4}$ (solid line), from [1].

Figure 4: Variations with t_α of the rotational E_ϕ, radial kinetic E_r, internal thermal E_ϵ, magnetis E_M energies, of the neutrino energy losses E_ν for $\alpha = 0.01$ (solid line) and $\alpha = 10^{-4}$ (dashed line). All the quantities are normalized to the maximum rotational energy $E_\phi^* = 10^{47}$ erg/cm per unit cylinder length, from [1].

the discontinuity front is the major source of neutrino emission (Fig.3). It is clear from Figs.3, 4 that the relationships between the variables (32) are little sensitive to decreasing α. The timescale growth proportional to $\alpha^{-1/2}$ is caused by an increase $\sim \alpha^{-1/2}$ in the number of turns of magnetic lines required for achieving the condition for the onset of runaway $\epsilon_M \sim \epsilon_G$. 2 illustates an increase in the number of turns with decreasing α for the same time t_α. Fig.4 demonstrates the conversion of the rotational energy into other energy forms.

Estimates based on the inclusion of the spherical gravitation potential of a real star and results of numerical computations give for the mass and energy of the shed material

$$M_{sh} \approx 0.13\, M_\odot, \quad \epsilon_{sh} \approx 0.035\, \epsilon_{rot} \tag{33}$$

which is valid only for small α; for $\alpha = 10^{-2}$ we have $\epsilon_{sh} \approx 0.08\, \epsilon_{rot}$. The major part of the envelope joins the core and rotates as a rigid body together with it. The angular velocity of the resulting model is $\sim 0.1\, V_0/R_0$, i.e. decreases by ~ 10 times relative to the initial velocity. Most of the initial rotational energy escapes in the form of neutrino emission, while most of the angular momentum is taken off by the ejected envelope. The parameter α has little effect on the integral neutrino flux $Q_\nu = \int_0^t \int_0^M f_\nu ds\, dt = \int_0^{t_\alpha} \int_0^M f_{\nu\alpha} ds\, dt_\alpha$.

An interesting result of calculations is a possible stage of magnetorotational oscillations of the core-envelope system, during which the angular velocity changes its sign. The angular velocity of the resulting core may be opposite to the initial angular velocity.

3.5 2-D calculations.

The attempt to obtain magneto-rotational explosion (MRE) in realistic 2-D picture have been done in [3]. The simpified problem was solved for initially uniform and rigidly rotating gas cloud and initial values of internal, rotational and magnetic energies taken as

$$\frac{E_{in0}}{|E_{gr0}|} = 0.1, \quad \frac{E_{rot0}}{|E_{gr0}|} = 0.04, \quad \frac{E_{magl}}{|E_{in1}|} = 0.05, \tag{34}$$

Here the index "0" is related to the initial state of the collapse, index "1" is related to the quasi-stationary state, which the rotating cloud without

magnetic field reaches in the process of collapse. The magnetic field was included into calculations in the point "1". This simplifies the calculations of the collapse and may be justified for a realistic case of the neutron star with $E_{magl}/E_{in1} \ll 1$, that it does not influence the process of the collapse. The dynamical action of the magnetic field begins to be important only after its considerable amplification in the process of twisting, which takes time much longer, then the time of the collapse and establishing of the quasi-stationary state. The quadrupole component of the magnetic field is expected to be the most important for MRE, because it has large radial component near the equator, which is amplified by the field twisting. In order to avoid a central singularity a regular field of the similar topology was chosen instead of the quadrupole in the form (in nondimensional variables)

$$
\begin{aligned}
H_{r1} &= F_r(0.5\,r,\ 0.5\,z - 2.5) - F_r(0.5\,r,\ 0.5\,z + 2.5) \\
H_{\phi 1} &= 0 \\
H_{z1} &= F_z(0.5\,r,\ 0.5\,z - 2.5) - F_z(0.5\,r,\ 0.5\,z + 2.5) \\
F_r(r,\,z) &= k\left(\frac{2rz}{(z^2+1)^3} - \frac{2r^3 z}{(z^2+1)^5}\right) \\
F_z(r,\,z) &= k\left(\frac{1}{(z^2+1)^2} - \frac{r^2}{(z^2+1)^4}\right)
\end{aligned}
\tag{35}
$$

Nondimensional variables in the equations (1)- (14) have been used with a factor

$$H_0 = \sqrt{P_0} = \rho_0^{1/2} r_0/t_0 \tag{36}$$

for the magnetic field components. The value $k = 0.43$ adjust the energy relation (34). The numerical method is based on the generalization of the implicit Lagrangian code to the case with a magnetic field [3]. On the outer boundary a nonzero value of the pressure $P_{out} = 10^{-3}P_0$ was keeped, which have not influenced the MRE process, but solved some numerical problems. At $r = 0$ it was assumed

$$v_r = v_\phi = B_r = B_\phi = (\nabla \times \mathbf{B})_r = (\nabla \times \mathbf{B})_\phi = 0 \tag{37}$$

and at $z = 0$

Figure 5: Triangular grid at t=23.929313.

Figure 6: Magnetic field patterns at t=23.937901.

$$v_z = B_z = \frac{\partial(\nabla \times \mathbf{B})_z}{\partial z} = 0 \tag{38}$$

was taken. The results of computations are presented in Figures 5 - 8

The quasi-stationary state in Fig.5 is presented at the moment very close to $t_1 = 23.920$, when the magnetic field (35) was included into computations. The magnetic field configuration (practically initial) at almost the same time is presented in Fig.6. Azimuthal component of the magnetic field increases until it becomes important for a dynamical influence. Magnetic pressure pushes out the matter, mainly in the equatorial plane, which expands and part of it (about 2.4 %) is flying away to the infinity, carring away about 0.5 % of the rotational energy of the configuration, formed after the collapse. Density contours and velocity fields, showing the development of the outburst are given Figs.7, 8.

Figure 7: Density contours and velocity field at t=39.779979.

Figure 8: Density contours and velocity field at t=46.113653.

4 Symmetry breaking of the magnetic field, anisotropic neutrino emission and high velocity neutron star formation

Observations of the pulsars moving at the velocities up to 500 km/s [27] is a challenge to the theory of the neutron star formation. The plausible explanation for the birth of rapidly mooving pulsars seems to be the suggestion of the kick at the birth from the asymmetric explosion. Make estimations for the strength of the kick, produced by the asymmetric neutrino emission during the collapse. The asymmetry of the neutrino pulse, is produced by the asymmetry of the magnetic field distribution, formed during the collapse and differential rotation.

Consider rapidly and differentially rotating new born neutron star with the dipole poloidal and symmetric toroidal fields. A field amplification during the differential rotation leads to the formation of an additional toroidal field from the poloidal one. This field, made from the dipole poloidal one by twisting is antisymmetric with respect to the symmetry plane. The sum of the initial symmetric with the induced antisymmetric toroidal fields has no plane symmetry.

In absence of dissipative processes the neutron star returns to the state of rigid rotation loosing the induced toroidal field and restoring mirror symmetry of the matter distribution. Formation of asymmetric toroidal field distribution is followed by magnetorotational explosion, which is asymmetric, leading to neutron star recoil and star acceleration [8]. The neutron star accelleration happens also [7] due to dependence of the cross-section of week interactions on the magnetic field.

In the magnetic field electrons occupy discret energy (Landau) levels for motion in the plane perpendicular to the field, with energy difference

$$\Delta\epsilon_L = \hbar\frac{eB}{m_e c}. \tag{39}$$

When this difference is of the order of the energy of beta decay Δ the decay probability begins to depend on the value of B. The critical magnetic field corresponds to

$$\Delta\epsilon_L = \lambda m_e c^2, \quad B_{cr} = \lambda \frac{m_e^2 c^3}{e\hbar} \simeq 4.4 \times 10^{13}\,\mathrm{Gs} \tag{40}$$

The probability of the neutron decay in the strong magnetic field was calculated in [34]

$$W_{nB} = W_n \left[1 + 0.17 \left(\frac{B}{B_{cr}}\right)^2 + ...\right] \quad \text{for } B \ll B_{cr} \tag{41}$$

and

$$W_{nB} = W_n\, 0.77 \left(\frac{B}{B_{cr}}\right) \quad \text{for } B > B_{cr} \tag{42}$$

with W_n is the probability for nonmagnetic case, see i.e. [6]. In strongly relativistic plasma with Fermi energy ε_{Fe} or kT larger then $\Delta > m_e c^2$ we should use in (40) a maximum between $\lambda = \frac{\epsilon_{Fe}}{m_e c^2}$ and $\lambda = \frac{kT}{m_e c^2}$.

After a collapse of rapidly rotating star the neutron star rotates at the period P about 1 ms. Differential rotation leads to the linear amplification of the toroidal field

$$B_\phi = B_{\phi 0} + B_p(t/P) \tag{43}$$

The time of the neutrino emission is several tens of seconds [33]. After 20 s the induced toroidal magnetic field will be about $2 \times 10^4 B_p$, corresponding to $10^{15} \div 10^{17}$ Gs for $B_p = 10^{11} \div 10^{13}$ Gs, observed in the pulsars. Adopting the initial toroidal field $B_{\phi 0} = (10 \div 10^3) B_p = 10^{12} \div 10^{16}$, we may estimate an asymmetry of the neutrino pulse. For symmetric $B_{\phi,0}$ and dipole poloidal field the difference ΔB_ϕ between the magnetic fields absolute values in two hemispheres increases, until it reaches the value $2B_{\phi 0}$. It remains constant later, while the relative difference

$$\delta_B = \frac{\Delta B_\phi}{B_{\phi+} + B_{\phi-}} \tag{44}$$

decreases. The main neutrino flux is formed in the region where the mean free path of the neutrino is smaller then the stellar radius. The quantity l_T having the meaning of the neutrino mean free path is connected with the neutrino opacity κ_ν as

$$\kappa_\nu = 1/(l_T \rho) \tag{45}$$

Calculations of the spherically symmetrical collaps [33] have shown, that during the phase of the main neutrino emission, a hot neutron star consists of the quasiuniform quasiisothermal core with the temperature T_i, whose mass increases with time, and the region between the neutrinosphere and the isothermal core, where the temperature smoothly decreases in about 10 times while the density, which finally drops about 6 times decreases non-monotonically. Neutrino flux is forming in this region, containing about one half of the neutron star mass. We suggest for sumplicity a power-law dependences for the temperature and l_T:

$$T = T_i \left(\frac{r_i}{r}\right)^m, \qquad l_T = \frac{1}{\kappa\rho} = l_{Ti}\left(\frac{r}{r_i}\right)^n \tag{46}$$

The neutrinosphere with the radius r_ν is determined approximately by the relation

$$\int_{r_\nu}^{\infty} \kappa_\nu \rho dr = \int_{r_\nu}^{\infty} \frac{dr}{l_T} = 1 \tag{47}$$

Using (46) outside the neutrinosphere we get from (47) the relation

$$r_\nu = r_i \left(\frac{r_i}{(n-1)l_{Ti}}\right)^{\frac{1}{n-1}} \tag{48}$$

Finally we get the temperature of the neutrinosphere T_ν and the neutrino luminosity L_ν

$$T_\nu = T_i \left(\frac{(n-1)l_{Ti}}{r_i}\right)^{\frac{m}{n-1}} \tag{49}$$

$$L_\nu = 4\pi r_\nu^2 H_\nu = \frac{7}{8} m \frac{16\pi a c T_i^4}{3} (n-1)^{\frac{4m-n+1}{n-1}} r_i^2 \left(\frac{l_{Ti}}{r_i}\right)^{\frac{4m-2}{n-1}} \tag{50}$$

To estimate the anisotropy of the neutrino flux we compare two stars with the same radius and temperature of the core r_i and T_i and different opacities. Let l_{Ti} is different and constant in two hemispheres, and each one is radiating according to (50). The anisotropy of the flux

$$\delta_L = \frac{L_+ - L_-}{L_+ + L_-} \tag{51}$$

here L_+, L_- are luminosities in the different hemispheres, calculated, using (50). For small difference between hemispheres

$$\delta_L = \frac{\Delta L}{L} = \frac{4m-2}{n-1}\frac{\Delta l_{Ti}}{l_{Ti}} \tag{52}$$

Here $n > 1$, when $m = \frac{1}{2}$ the neutrino fluxes in both hemispheres are equal because smaller opacity and larger neutrinosphere temperature T_ν from (49) is compensated by smaller neutrinosphere radius r_ν from (48). The equation of motion of the neutron star with the mass M_n

$$M_n\frac{dv_n}{dt} = \frac{L_+ - L_-}{c}, \qquad L_+ + L_- = \frac{2}{\pi}L_\nu(t) \tag{53}$$

For the power distributions it follows from (50) that

$$L_\pm = A l_{Ti\pm}^{\frac{4m-2}{n-1}} \tag{54}$$

As an example consider the dependence on B in the form (41),(42) . Making interpolation between two asimptotic forms we get dependence

$$l_{Ti\pm} \sim \frac{1}{W} = l_{T0}\frac{1+\left(\frac{B}{B_c}\right)^3}{1+0.17\left(\frac{B}{B_c}\right)^2+0.77\left(\frac{B}{B_c}\right)^4} = l_{T0}F^{\frac{n-1}{4m-2}}(B) \tag{55}$$

The time dependence of the average value of B in each hemisphere can be found from (43) with

$$B_{p+} = -B_{p-}, \quad B_{\phi 0+} = B_{\phi 0-} \tag{56}$$

By B_p we mean a radial component of the poloidal field taking part in amplification of B_ϕ. The time dependence of L_ν is taken from the spherically symmetric calculations of the collapse.

For $\frac{4m-2}{n-1} = 1$ and in condition when the neutron star is accelerated at $B \gg B_c$, we have $F_\pm = \frac{B_c}{0.77B_\pm}$. Equation of motion (53) may be written as

$$M_n\frac{dv_n}{dt} = \frac{2}{\pi}\frac{L_\nu}{c}\frac{|B_+| - |B_-|}{|B_+| + |B_-|} \tag{57}$$

with the linear functions for $B_{\pm}$. Take constant $L_\nu = \frac{0.1 M_n c^2}{20 s}$. With these simplifications, the final velocity of the neutron star v_{nf} follows as a result of the solution of (57) in the form

$$v_{nf} = \frac{2}{\pi} \frac{L_\nu}{M_n c} \frac{P B_{\phi 0}}{|B_p|} (0.5 + \ln\left(\frac{20\, s}{P} \frac{|B_p|}{B_{\phi 0}}\right)) \tag{58}$$

For $P = 10^{-3}\, s$ we obtain

$$v_{nf} = \frac{2}{\pi} \frac{c}{10} \frac{P}{20\, s} x (0.5 + \ln(\frac{20\, s}{P} \frac{1}{x})) \approx 1 \frac{km}{s} x (0.5 + \ln \frac{2 \times 10^4}{x}) \tag{59}$$

For the value $x = \frac{B_{\phi 0}}{|B_p|}$ ranging between 20 and 10^3, we have v_{nf} between 140 and 3000 km/s, what can explain the nature of the most rapidly mooving pulsars. The formula (59) can be applied when $B_{\phi 0} \gg B_c$ and $x \gg 1$.

The acceleration of the collapsing star by anisotripic neutrino emission can happen even when the star collapses to the black hole, the efficiensy of acceleration decreases with increasing of mass. We may expect black holes of stellar origin moving rapidly, like radiopulsars, and they may be found high over the galactic disk. This is observed among the soft X ray novae - most probable candidates for black holes in the Galaxy.

References

[1] Ardelyan,N.V., Bisnovatyi-Kogan,G.S., Popov,Yu.P. (1979) Astron.Zh **56** 1244

[2] Ardelyan,N.V., Bisnovatyi-Kogan,G.S., Popov,Yu.P., Chernigovskii,S.V. (1987) Astron.Zh. **64** 495

[3] Ardeljan,N.V., Bisnovatyi-Kogan,G.S., Moiseenko S.G. (1995) Ap.Space Sci. **239** 1

[4] Arnett,D., (1967) Canad.J.Phys **45** 1621

[5] Bisnovatyi-Kogan,G.S.(1970) Astron.Zh. **47** 813

[6] Bisnovatyi-Kogan,G.S.(1989) *Physical Problems of Theory of Stellar Evolution.* (M. Nauka)

[7] Bisnovatyi-Kogan,G.S. (1993) Astron. Ap. Transact. **3** 287

[8] Bisnovatyi-Kogan,G.S., Moiseenko,S.G. (1992) Sov. Astron. **36** 285

[9] Bisnovatyi-Kogan,G.S., Popov,Yu.P., Samochin,A.A. (1976) Ap.Space Sci. **41** 321

[10] Blinnikov,S.I., Lozinskaya,T.A., Chugai,N.N. (1987) Itogi Nauki i Tekhniki, Astronomiya **32** 142

[11] Burrows,A. (1987) ApJ Lett. **318** L57

[12] Burrows,A., Fryxell,B.A. (1993) ApJ Lett. **418** L33

[13] Burrows,A., Hayes,J., Fryxell,B.A. (1995) ApJ **450** 830

[14] Colgate,S., White,R. (1966) ApJ **143** 626

[15] Epstein,R.I. (1979) Month.Not.R.A.S. **188** 305

[16] Herant,M., Benz,W., Hix,W.R., Fryer,C.L., Colgate,S.A. (1994) ApJ **435** 339

[17] Hillebrandt,W. (1985) Proc. NATO-ASI High energy phenomena around collapsed stars, Cargese

[18] Imshennik,V.S., Nadyozhin,D.K. (1982) Itogi Nauki i Tekhniki, Astronomiya **21** 63

[19] Ivanova,L.N., Imshennik,V.S., Nadyozhin,D.K. (1969) Nauch.Inf., Issue 13, 3

[20] Janka,H.-T., Müller,E. (1994) Astron.Ap. **290** 496

[21] Janka,H.-T., Müller,E. (1995) ApJ Lett. **448** L109

[22] Lamb,D.Q., Lattimer,J.M., Pethick,C.J., Ravenhall,D.G. (1978) Phys.Rev. Lett. **41** 1623

[23] Landau,L.D., Lifshitz,E.M. (1982): *Electrodynamics of Continua* (M., Nauka)

[24] Lattimer,J., Mazurek,T.(1981) ApJ **246** 955

[25] Lattimer,J., Mazurek,T. (1980) Proc. DUMAND-1980

[26] Le Blank,L.M., Wilson,J.R. (1970) ApJ **161** 541

[27] Lyne,A.G., Lorimer,D.R. (1994) Nature **369** 127

[28] Mayle,R., Wilson,J.R., Schramm,D.N. (1987) ApJ **318** 288

[29] Müller,E., Hillebrandt,W. (1979) Astron.Ap. **80** 147

[30] Miller,D.S., Wilson,J.R., Mayle,R.W. (1993) ApJ **415** 278

[31] Nadyozhin,D.K. (1977) Ap. Space Sci. **49** 399

[32] Nadyozhin,D.K. (1977) Ap. Space Sci. **51** 284

[33] Nadyozhin,D.K. (1978) Ap. Space Sci. **53** 131

[34] O'Connell, R.F., Matese,J.J. (1969) Nature **222** 649

[35] Ohnishi,T. (1983) Tech.Rep. Inst.At. En.Kyoto Univ. No. 198

[36] Shimizu,T., Yamada,S., Sato,K. (1994) ApJ Lett. **432** L119

[37] Shklovski,I.S. (1976): *Supernovae Stars* (M., Nauka)

[38] *Supernova 1987A*, in Proc. workshop ESO, July 1987.

[39] Van den Hulst,J., et al. (1983) Nature **306** 566

[40] Wilson,J.R., Mayle,R., Woosley,S., Weaver,T. (1986) Ann. N-Y Acad. Sci. **470** 267

[41] Woosley,S., Weaver,T. (1986) in *Nucleosynthesis and its implications on nuclear and particle physics* ed. J. Audouze, N. Mathieu (D. Reidel) p. 145

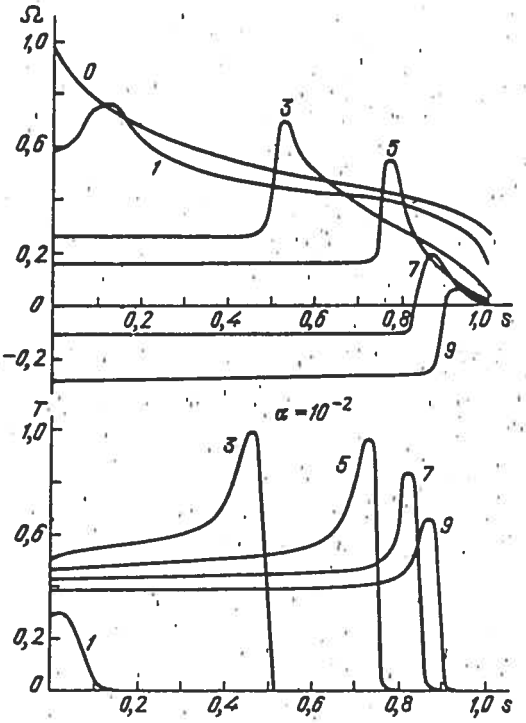

Fig 1

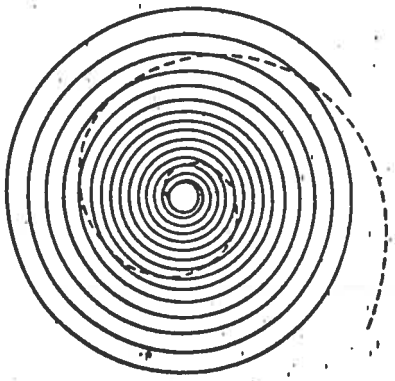

Fig. 2

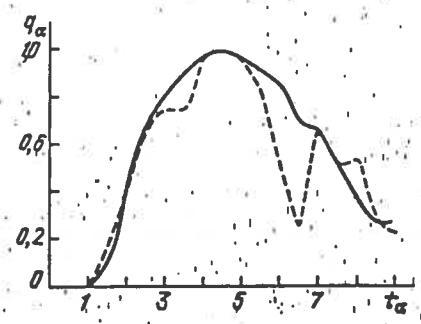

Fig. 3

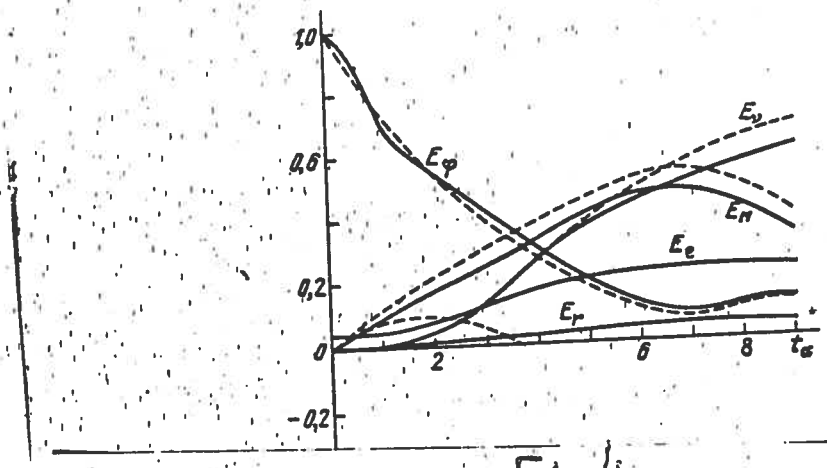

Fig 4

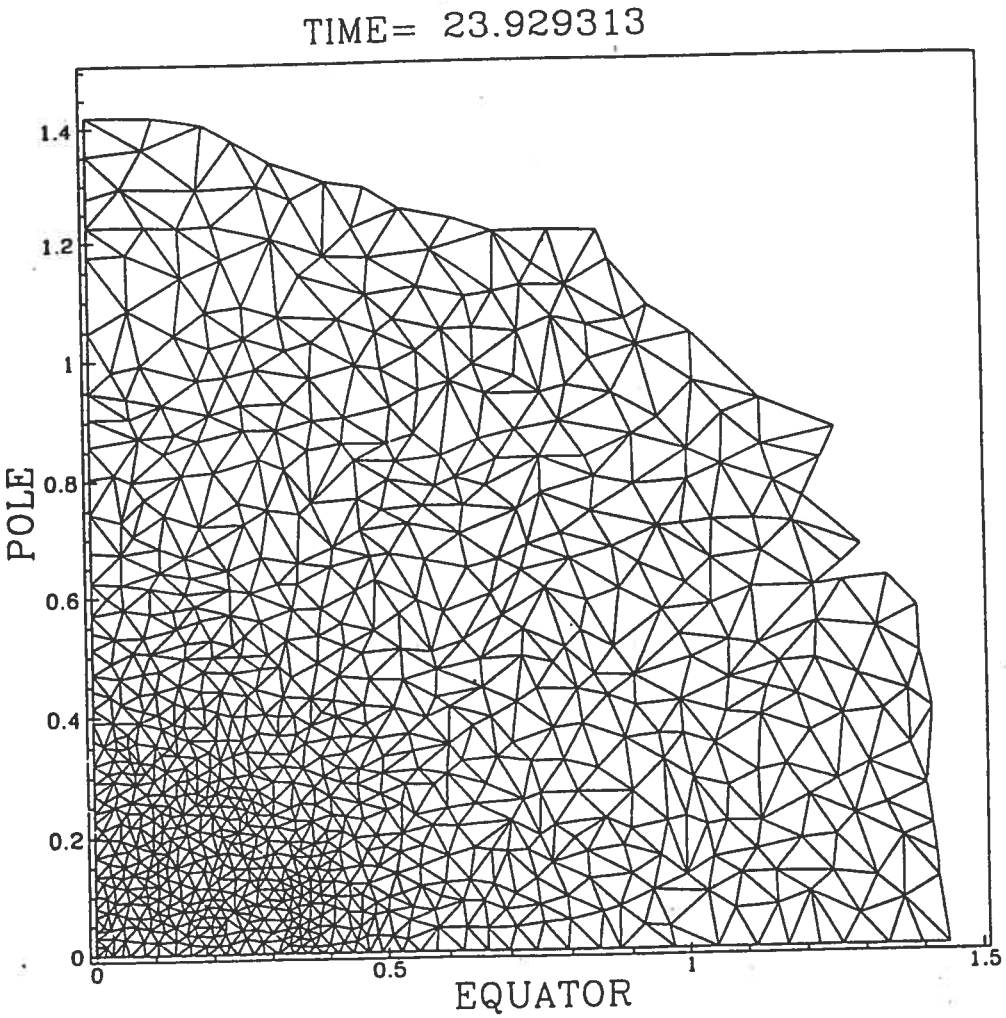

Fig.5

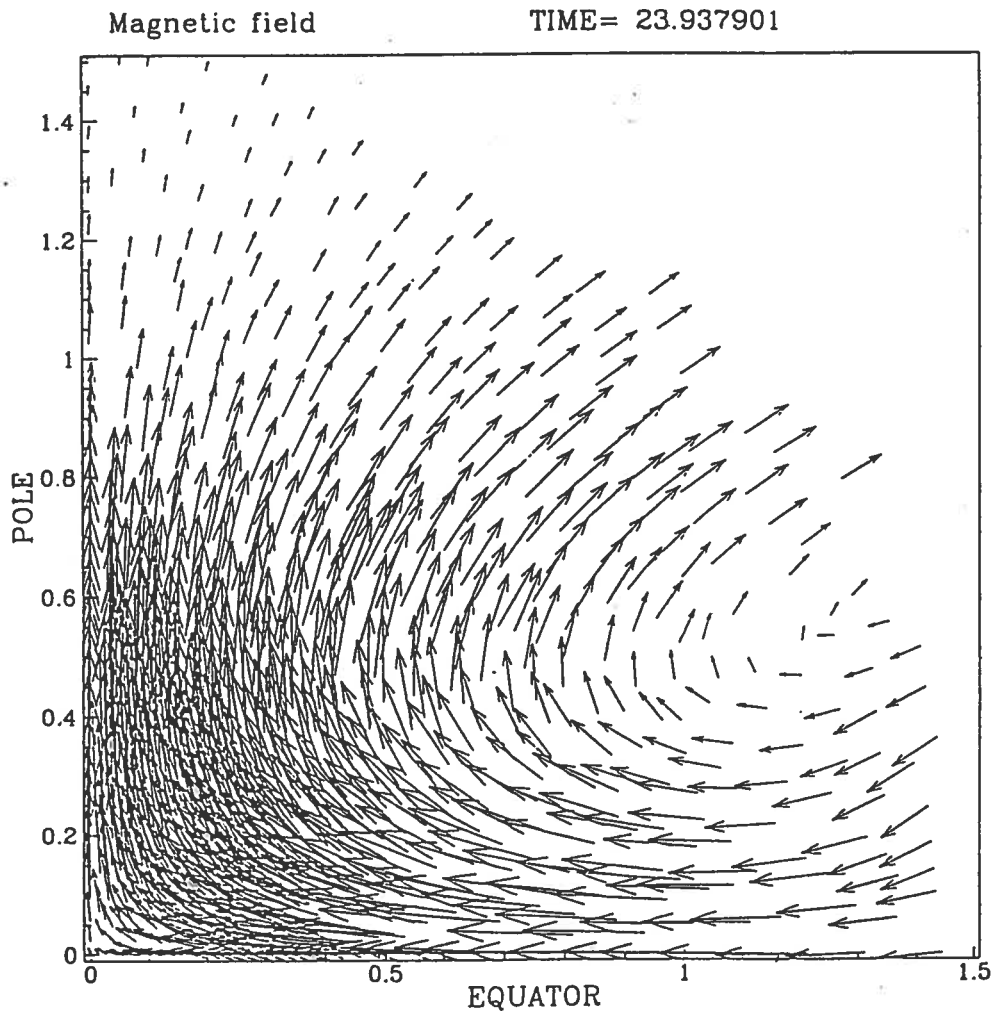
Magnetic field
TIME= 23.937901
POLE
EQUATOR
0
0.2
0.4
0.6
0.8
1
1.2
1.4
0.5
1.5

Fig. 6

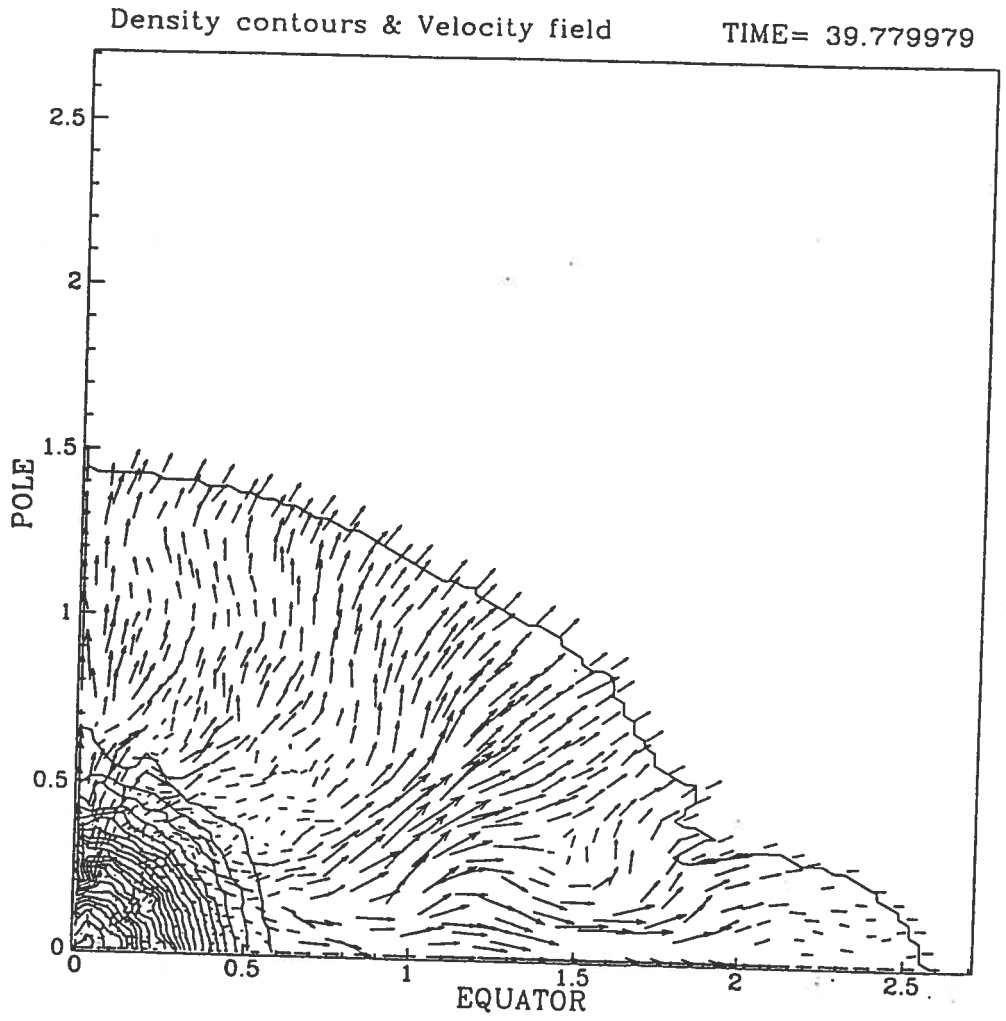
Density contours & Velocity field
TIME= 39.779979
POLE
EQUATOR
0
0.5
1
1.5
2
2.5
1 - 0.000842
2 - 0.840287
3 - 1.679731
4 - 2.519176
5 - 3.358620
6 - 4.198065
7 - 5.037509
8 - 5.876954
9 - 6.716398
10 - 7.555843
11 - 8.395288
12 - 9.234732
13 - 10.074177
14 - 10.913621
15 - 11.753065
16 - 12.592510
17 - 13.431954
18 - 14.271399
19 - 15.110845
20 - 15.950288
21 - 16.789734
22 - 17.629179
23 - 18.468622
24 - 19.308067
25 - 20.147512

Fig. 7

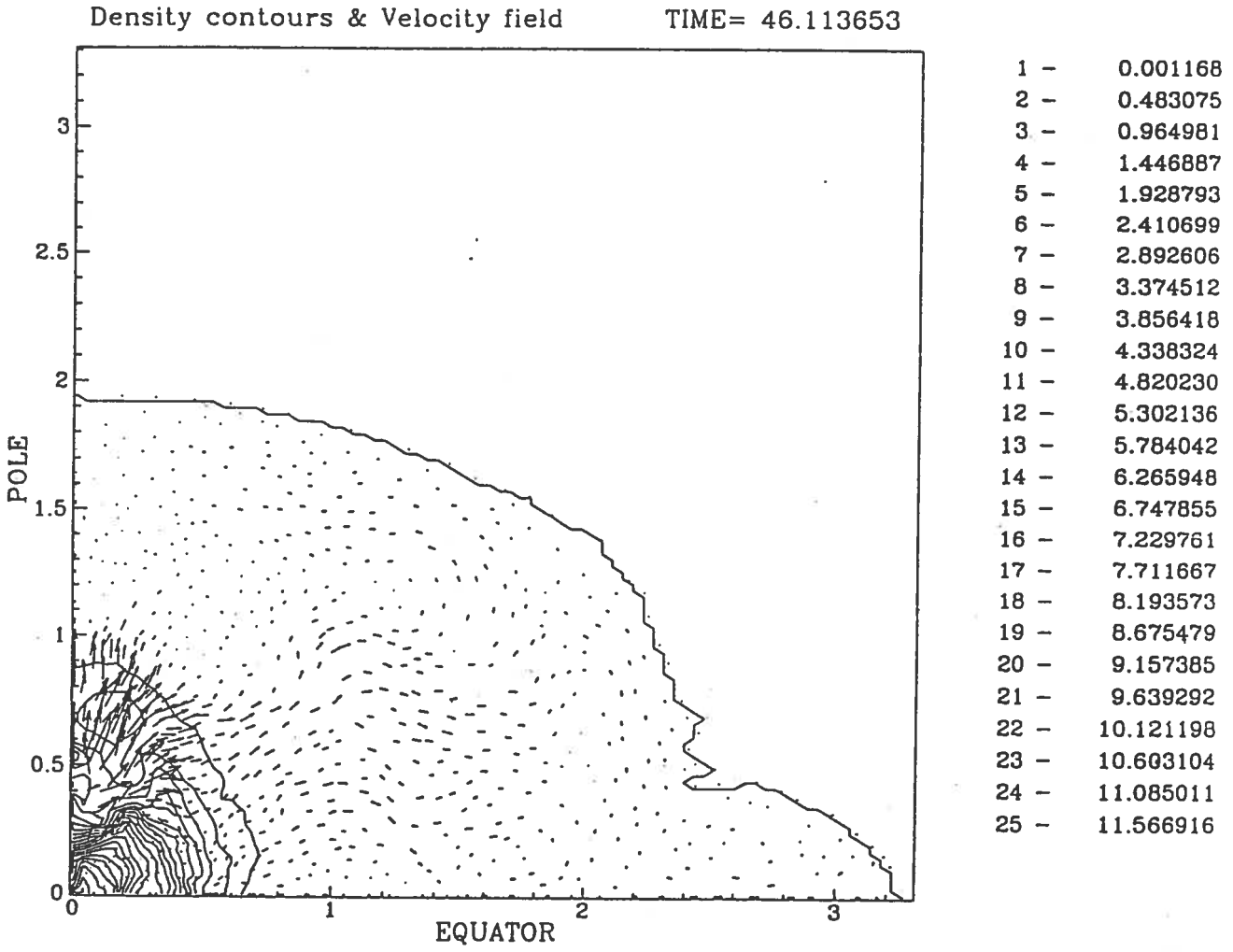
Density contours & Velocity field
TIME= 46.113653
POLE
EQUATOR
0
0.5
1
1.5
2
2.5
3
0
1
2
3
1 – 0.001168
2 – 0.483075
3 – 0.964981
4 – 1.446887
5 – 1.928793
6 – 2.410699
7 – 2.892606
8 – 3.374512
9 – 3.856418
10 – 4.338324
11 – 4.820230
12 – 5.302136
13 – 5.784042
14 – 6.265948
15 – 6.747855
16 – 7.229761
17 – 7.711667
18 – 8.193573
19 – 8.675479
20 – 9.157385
21 – 9.639292
22 – 10.121198
23 – 10.603104
24 – 11.085011
25 – 11.566916

Fig. 8